Polymer Journal, Vol. 16, No. 10, pp 771—778 (1984)

Dynamical Properties of Polymer Solutions from Θ to Critical Regions as Measured by Quasi-Elastic Light Scattering: Polystyrene–Methylcyclohexane System

Masato TAKAHASHI and Takuhei NOSE

Department of Polymer Chemistry, Tokyo Institute of Technology, Ookayama, Meguro-ku, Tokyo 152, Japan

(Received May 11, 1984)

ABSTRACT: Static and dynamic light scattering was measured for methylcyclohexane solutions of polystyrene with molecular weights 1.75×10^4, 5.00×10^4, 1.10×10^5, 2.33×10^5, 4.22×10^5, and 1.26×10^6 in the temperature region from Θ to the critical point. It was found that the average line width $\bar{\Gamma}$ for higher molecular weights deviated from the prediction of the mode–mode coupling theory, showing a large background whose temperature dependence apparently had the same trend as that of small molecule systems. The decay of the correlation function was more non-exponential for higher molecular weight. A histogram analysis showed that the line width distribution was bimodal for higher molecular weights of 4.22×10^5 and 1.26×10^6.

KEY WORDS Dynamic Light Scattering / Critical Phenomena / Polymer Solution / Polystyrene / Methylcyclohexane /

Critical phenomena in polymer solutions have been studied by many workers[1-12] with interest directed primarily toward critical exponents and the molecular weight dependence of critical amplitudes. Most investigations, however, have been limited to static properties such as correlation length, isothermal osmotic compressibility, coexistence curve and interfacial tension. Dynamical critical phenomena in polymer solutions have not as yet been investigated extensively, except for a few studies by Kuwahara *et al.*[5,6,12]

Generally, the Rayleigh line width Γ observed in the vicinity of the critical temperature is separated into the background part Γ_B and the critical part Γ_C:

$$\Gamma=\Gamma_B+\Gamma_c$$

The critical part Γ_C is usually represented by the mode-mode coupling theory of Kawasaki,[13] *i.e.*,

$$\Gamma_C/k^3=\frac{k_BT}{8\pi\eta^*}(k\xi)^{-3}[1+(k\xi)^2+\{(k\xi)^3-(k\xi)^{-1}\}\tan^{-1}(k\xi)] \quad (1)$$

where $k=(4\pi/\lambda)\sin(\theta/2)$ with λ and θ being the wavelength of light in the scattering medium and the scattering angle, respectively, k_B the Boltzmann constant, T the absolute temperature, η^* the viscosity, and ξ the correlation length. In the hydrodynamic region ($k\xi<1$), eq 1 is reduced to $\Gamma_C/k^3\sim(k\xi)^{-1}$, *i.e.*,

$$D=\Gamma_C/k^2\propto\xi^{-1} \quad (2)$$

where D is the diffusion coefficient. On the other hand, in the non-hydrodynamic region ($k\xi>1$), eq 1 leads to

$$\Gamma_C/k^3=\text{const} \quad (3)$$

The background part Γ_B was examined in detail by Swinney and Henry[14] and by Oxtoby and Gelbart.[15] According to the re-

sults of Oxtoby and Gelbart, Γ_B in the hydrodynamic region changes with temperature as $\Gamma_B/\Gamma_C \propto t^{\nu}$, so that

$$\Gamma = \Gamma_C + \Gamma_B = \Gamma_C(1 + At^{\nu})$$
$$= \Gamma_{CO} t^{\nu}(1 + At^{\nu}) \quad (4)$$

where

$$t \equiv |T - T_c|/T_c$$

with T_c the critical temperature, ν the critical exponent of the correlation length, Γ_{CO} the critical amplitude of Γ_C, and A a constant associated with shear viscosity. Hamano *et al.*[12] studied dynamical critical phenomena for a polydimethylsiloxane–diethyl carbonate mixture, and found the background part of the line width in this polymer solution to be similar to those of small molecule systems.

Munch *et al.*[16] measured the hydrodynamic correlation length ξ_H for polystyrene in cyclohexane in the temperature range from Θ to the critical region and found that ξ_H had a stronger temperature dependence than the theoretical prediction. That is, the critical exponent of ξ_H, ν_H, defined by $\xi_H \propto t^{-\nu_H}$ was 0.73 for $M_w = 2 \times 10^6$ and 0.79 for $M_w = 1.3 \times 10^5$, both larger than the theoretical value $\nu_H = 0.63$. They concluded that their experimental results for molecular-weight (M) dependence of the critical amplitude ξ_{HO} for ξ_H was in reasonable agreement with their theoretical prediction $\xi_{HO} \propto M^{1/6}$. However, the critical amplitude of the static correlation length ξ_0 is known to obey $\xi_0 \sim M^{1/4}$.[2,3,4,9,10]

The critical concentration of a polymer solution is of the order of the overlap concentration C^*.[17] At concentrations comparable to or higher than C^*, the correlation function near the Θ-temperature shows a bimodal decay even in the region of $kR_g < 1$.[18] Thus, the profile of the correlation function should be taken in a consideration of the dynamical behavior near the critical point in polymer solutions.

In this work, the dynamical behavior of critical solutions in the temperature region from Θ to the critical point, was investigated by measuring the static and dynamic light scattering of methylcyclohexane solutions of polystyrene (PS) with different molecular weights. The average line width $\bar{\Gamma}$ was compared with the mode–mode coupling theory (eq 1—3), and the background part in $\bar{\Gamma}$ was evaluated by eq 4. The profile of the correlation function was interpreted in terms of the line-width distribution function estimated by the histogram method.

EXPERIMENTAL

A. Sample

We used Pressure Chemical polystyrenes with $M_w = 1.75 \times 10^4$, 5.00×10^4, 1.10×10^5, and 2.33×10^5 ($M_w/M_n < 1.06$) and Toyo Soda polystyrenes with $M_w = 4.22 \times 10^5$ ($M_w/M_n = 1.04$) and $M_w = 1.26 \times 10^6$ ($M_w/M_n = 1.05$). Methylcyclohexane of spectroscopic grade was purified by fractional distillation after dehydration with calcium hydride.

Coexistence curves for these polystyrenes except for that with $M_w = 4.22 \times 10^5$ were measured in previous studies,[10,11] where the critical concentration ϕ_c was determined at an intersection of the coexistence curve and the diameter on which the volume ratio of one separated phase to the other is unity. No appreciable effect of polydispersity on the phase diagram was found. ϕ_c for $M_w = 4.22 \times 10^5$ was determined in the present experiment by the same method. The values of ϕ_c in volume fraction are listed in Table I.

Dust particles in solutions were removed by a Milipore filter (nominal diameter = 0.22 μm) for lower molecular weights and by centrifugation for higher molecular weights. Solutions with critical concentrations were flame-sealed in light scattering cells having a light path length of 10 mm or 5 mm.

B. Apparatus

Static and dynamic light scattering was mea-

sured by a specially designed photometer with an argon-ion laser source (Nippon Electric Co., model GLG 3200) operating at wavelength 488 nm. A He–Ne laser (Nippon Electric Co., model GLG 2040) with wavelength 633 nm was also used in some dynamic measurements. The single clipped photoelectron count auto-correlation function $G^{(2)}(\tau)$ was measured by a 48-channel Malvern digital correlator (K7023). The temperature was controlled to within ± 0.01°C. The range of scattering angle was from 30° to 150° for static measurements, and from 70° to 110° for dynamic measurements. We used benzene as a reference for computing the Rayleigh ratio of samples and chose 3.20×10^{-5} $[1+0.368\times10^{-2}(T/\mathrm{K}-298.15)]$ cm^{-1} as the Rayleigh ratio of benzene at the scattering angle 90° for vertically polarized incident and scattered light at a wavelength of 488 nm and temperature T.[18]

C. *Methods of Data Analysis*

Attenuation correction was made for measured scattered intensities I_{meas}, which are related to the true scattered intensities I by $I_{\mathrm{meas}}=I\exp(-\tau_{\mathrm{b}}d)$, where τ_{b} is the turbidity of the solution and d the light path length. τ_{b} was estimated by

$$\tau_{\mathrm{b}}=I_0\pi\left[\frac{2\alpha^2+2\alpha+1}{\alpha^3}\ln(1+2\alpha)-\frac{2(1+\alpha)}{\alpha^2}\right] \tag{5}$$

where I_0 is the scattered intensity extrapolated to zero angle, and $\alpha=2(k_0\xi)^2$ with k_0 the wave number of incident light.[19] The maximum correction was about 50%.

The correlation length ξ and the scattered intensity at zero angle I_0 were calculated from the Ornstein–Zernike–Debye theory[20]

$$I_0/I(\theta)=1+k^2\xi^2 \tag{6}$$

The critical temperature T_{c} was determined by a least-squares fitting of I_0/T to

$$I_0/T=(I_0/T)_0t^{-\gamma} \tag{7}$$

where γ is the critical exponent of isothermal osmotic compressibility and $(I_0/T)_0$ the critical amplitude of I_0/T. The critical temperarure thus obtained are listed in Table I. The temperature dependence of the correlation length ξ was described by

$$\xi=\xi_0t^{-\nu} \tag{8}$$

where ξ_0 and ν are the critical amplitude and critical exponent of ξ, respectively.

The normalized correlation function $g^{(1)}(\tau)$ of the scattered electric field was calculated from measured $G^{(2)}(\tau)$ using the relation

$$G^{(2)}(\tau)=B(1+\beta|g^{(1)}(\tau)|^2) \tag{9}$$

where B is the background and β a parameter for data fitting. The correlation function $g^{(1)}(\tau)$ was analyzed by the cumulant method[21] to obtain an average line width $\bar{\Gamma}$ and its variance $\mu_2/\bar{\Gamma}^2$, where

$$|g^{(1)}(\tau)|=\int_0^\infty G(\Gamma)\exp(-\Gamma\tau)\,\mathrm{d}\Gamma \tag{10}$$

with

$$\bar{\Gamma}=\int_0^\infty \Gamma G(\Gamma)\,\mathrm{d}\Gamma \tag{11}$$

and

$$\mu_i=\int_0^\infty (\Gamma-\bar{\Gamma})^iG(\Gamma)\,\mathrm{d}\Gamma \tag{12}$$

Here, $G(\Gamma)$ is the normalized distribution function of the line width Γ. The diffusion coefficient D in the hydrodynamic region was calculated by

$$D=\bar{\Gamma}/k^2 \tag{13}$$

from the average line width $\bar{\Gamma}$. $G(\Gamma)$ was estimated by the histogram method,[22] where

$$g^{(1)}(\tau)=\sum_{j=1}^{n} G(\Gamma_j)\int_{\Gamma_j-\Delta\Gamma/2}^{\Gamma_j+\Delta\Gamma/2}\exp(-\Gamma\tau)\,\mathrm{d}\Gamma \tag{14}$$

with the normalization condition

$$\sum_{j=1}^{n} G(\Gamma_j)\Delta\Gamma=1 \tag{15}$$

n is the number of steps in the histogram, $G(\Gamma_j)$ the histogram from $\Gamma=\Gamma_j-\Delta\Gamma/2$ to $\Gamma=\Gamma_j+\Delta\Gamma/2$, and $\Delta\Gamma$ the width of each step. The average line width and the i-th moment are respectively given by

$$\bar{\Gamma}=\sum_{j=1}^{n}\Gamma_j G(\Gamma_j)\Delta\Gamma \tag{16}$$

and

$$\mu_i=\sum_{j=1}^{n}(\Gamma_j-\bar{\Gamma})^i G(\Gamma_j)\Delta\Gamma \tag{17}$$

RESULTS AND DISCUSSION

A. *Critical Exponent and Molecular Weight Dependence of the Diffusion Coefficient*

The t-dependence of the correlation length ξ is described by eq 8 with the values of ν listed in Table I, which are somewhat smaller than the theoretical value by the non-classical treatment,[23] $\nu=0.63$.

The $\bar{\Gamma}$ values with the background not subtracted were proportional to k^2 in the hydrodynamic region for all molecular weights. Figure 1 shows an example of $\bar{\Gamma}$ *vs.* k^2 plot. Diffusion coefficients D calculated from the $\bar{\Gamma}$ values by eq 13 in the hydrodynamic region are shown in Figure 2 for some molecular weights in the temperature region of $0.004\leq t\leq 0.013$. The least-squares fitting to the power law

$$D=D_0 t^{\nu'}$$

gave the critical exponent ν' the values listed in Table I. The values of ν' in this t-region are close to ν from the static correlation length. However, as shown in Figure 3, the diffusion coefficient D did not follow the power law $D\sim t^{\nu'}$ in any of the experimental range of t for $M_w\geq 2.33\times 10^5$. The slope (ν') of a

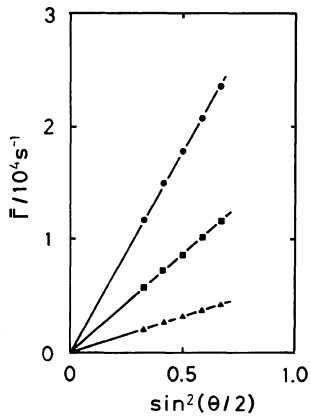

Figure 1. Angular dependence of average line widths $\bar{\Gamma}$ for $M_w=2.33\times 10^5$. (●), 344.34 K; (■), 334.32 K; (▲), 328.19 K.

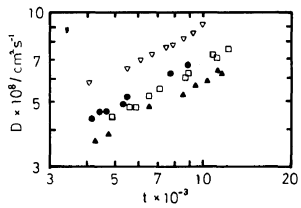

Figure 2. Temperature dependence of diffusion coefficients D in the temperature range of $0.004\leq t\leq 0.013$ for $M_w=1.75\times 10^4$ (▽), 5.00×10^4 (●), 2.33×10^5 (□) and 4.22×10^5 (▲).

Table I. Values of ϕ_c, T_c, exponents ν, ν', ν'', and A

M_w / 10^5	ϕ_c / ml ml^{-1}	T_c / K	ν	ν'	ν''	A
0.175	0.169	295.38	0.54±0.08	0.50±0.08	—	—
0.500	0.111	312.40	0.65±0.08	0.56±0.05	—	—
1.10	0.0843	321.74	0.67±0.06	0.63±0.08	—	—
2.33	0.0610	328.15	0.54±0.04	0.60±0.05	0.57	5.34
4.22	0.0517	332.30	0.54±0.04	0.54±0.08	0.58	5.79
12.6	0.0289	337.35	0.58±0.04	0.64±0.08	0.54	5.34

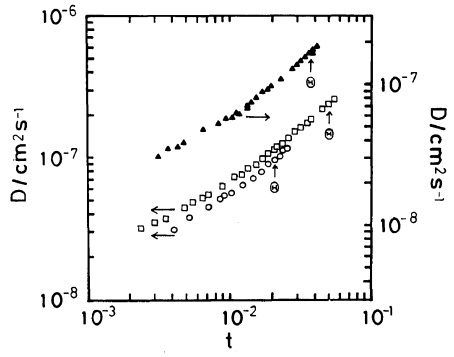

Figure 3. Temperature dependence of diffusion coefficients in the whole experimental range of t for $M_w = 2.33 \times 10^5$ (□), 4.22×10^5 (▲), and 1.26×10^6 (○).

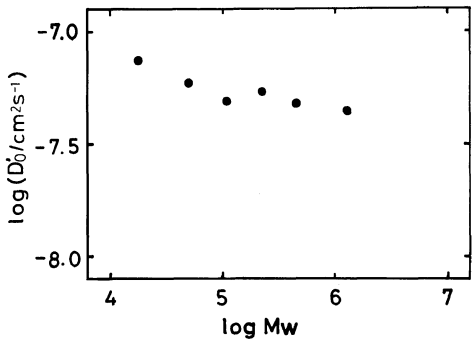

Figure 4. Molecular weight dependence of D_0' (D at $t = 0.007$).

$\log D - \log t$ plot decreases with decreasing t and approaches v defined by $\xi \sim t^{\nu}$. Therefore, the mean value of ν' for the entire t-range is larger than ν, consistent with the result of Candau *et al.*,[16] this suggests that D does not obey the relation $D \sim \xi^{-1}$ in any part of the range of t.

Figure 4 shows a double logarithmic plot of the diffusion coefficient at a fixed t-value ($t = 0.007$), D_0', against molecular weight, indicating a molecular weight dependence of the critical amplitude of D. A least-squares fitting to this plot gave

$$D_0' \sim M^{-0.11} \tag{18}$$

We also obtained $\eta^* \xi_{HO} \propto k_B T / D_0' \propto M^{0.14}$ by a least-squares fitting, where $\xi_{HO} = k_B T / 6\pi\eta^* D_0'$ and T is the temperature at $t = 0.007$ which depends on M. The exponent 0.14 is consistent with the suggestion of Candau *et al.*[16] for the exponent of $\xi_{HO}(1/6)$, since they regarded η^* as the solvent viscosity independent of M. However, this exponent value is lower than the index for the molecular weight dependence of $\xi_{HO}(1/4)$.[2,3,4,9,10] This may be due to the molecular weight dependence of η^* and the background in line width.

B. *Comparison with the Kawasaki Function*

Figure 5 shows plots of $\bar{\Gamma}/k^3$ *vs.* $k\xi$, where the solid curve represents the mode–mode coupling theory (eq 1).[13] Here, since no data of viscosity η^* were available, the theoretical curve was shifted along the ordinate to the experimental data in the region of $k\xi > 1$. Agreement between experiment and theory is good for lower molecular weights ($M_w \leq 1.10 \times 10^5$). However, as the molecular weight increases, departure from theory becomes apparent and more appreciable, probably because of the contribution of the background. The breakdown of the relation $\bar{\Gamma}/k^2 \propto \xi^{-1}$ in the hydrodynamic region is responsible for the disagreement with the mode–mode coupling theory, since the $\bar{\Gamma}$ exhibits a k^2-dependence, *i.e.*, $\bar{\Gamma}/k^3 \propto k^{-1}$. Thus, $\bar{\Gamma}/k^3 \propto (k\xi)^{-1}$ at fixed k (*i.e.*, $\bar{\Gamma} \propto \xi^{-1}$) does not hold, as already suggested in the last section.

C. *Background in Line Width*

The breakdowns of the power law for D and the relation $D \sim \xi^{-1}$ found in the hydrodynamic region may be due to the background in $\bar{\Gamma}$. Hence, the background part of the average line width $\bar{\Gamma}$ was determined by a least-squares fitting to eq 4, with A and ν taken as parameters. The resulting values of A and critical exponent (denoted by ν'') are listed in Table I. Agreement between ν'' from the background evaluation and ν from the static correlation length is fairly good for $M_w = 2.33 \times 10^5$, 4.22×10^5, and 1.26×10^6. Therefore, the background part of line width $\bar{\Gamma}$ can be described by eq 4, as found in systems of small mol-

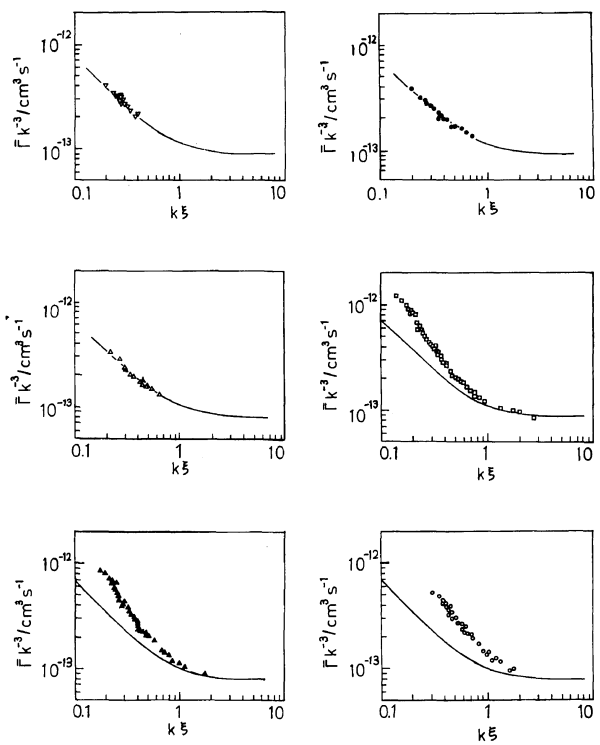

Figure 5. Plots of $\bar{\Gamma}/k^3$ *vs.* $k\xi$ for $M_w = 1.75 \times 10^4$ (▽), 5.00×10^4 (●), 1.10×10^5 (△), 2.33×10^5 (□), 4.22×10^5 (▲) and 1.26×10^6 (○).

ecules.[14,15] The contribution of the background part to the line width (At^v) was about 40% at $t \sim 0.01$ and about 15% at $t \sim 0.002$. The background part evaluated by Kuwahara[12] for polydimethylsiloxane ($M_w = 8.0 \times 10^4$) was 4.9% at $t = 3.22 \times 10^{-4}$ and 0.6% at $t = 9.75 \times 10^{-6}$.

D. *Profile of the Correlation Function*

In previous sections we discussed the average line width $\bar{\Gamma}$. Measured auto-correlation functions exhibited a non-exponential decay for higher molecular weights, as seen from Figure 6 for $\mu_2/\bar{\Gamma}^2$. The variance $\mu_2/\bar{\Gamma}^2$ increased with increasing molecular weight. Thus, the value of $\mu_2/\bar{\Gamma}^2$ for $M_w = 1.26 \times 10^6$, 4.22×10^5, 2.33×10^5 and 1.10×10^5 were about 1.25, 0.65, 0.3 and less than 0.1, respectively, showing no clear temperature dependence. Because a non-single exponential

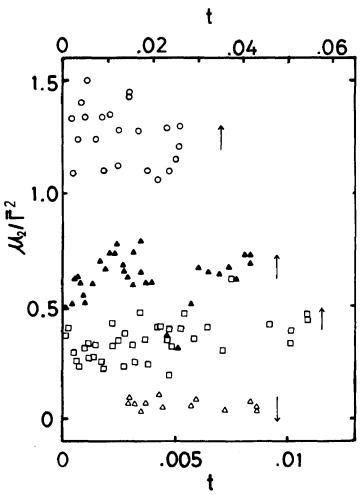

Figure 6. Temperature dependence of $\mu_2/\bar{\Gamma}^2$. Symbols are the same as those in Figure 5.

decay was obtained, the agreement of $\bar{\Gamma}$ with eq 4 may be apparent, and a detailed analysis

Table II. Values of $\bar{\Gamma}$ and $\mu_2/\bar{\Gamma}^2$ by the cumurant method (cu) and histogram method (h)

M_w / 10^5	t	$\bar{\Gamma}_{cu}$ / s^{-1}	$\bar{\Gamma}_h$ / s^{-1}	$(\mu_2/\bar{\Gamma}^2)_{cu}$	$(\mu_2/\bar{\Gamma}^2)_h$
1.10	3.67×10^{-3}	1400	1408	0.07	0.02
4.22	1.87×10^{-2}	8600	8218	1.16	0.58
12.6	1.46×10^{-2}	4850	4974	1.43	1.05

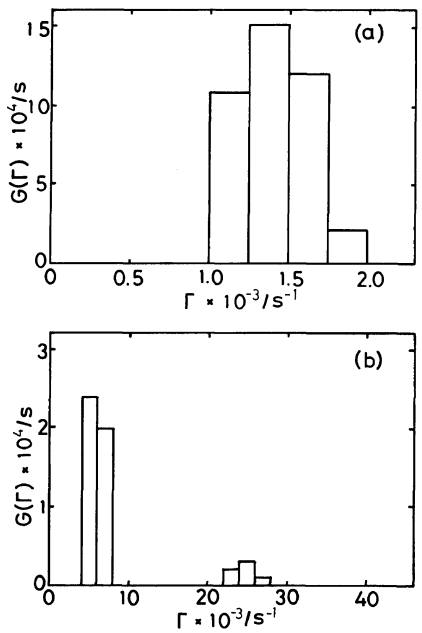

Figure 7. Line width distribution function $G(\Gamma)$ obtained by histogram analysis for $M_w=1.10\times10^5$ at $t=3.67\times10^{-3}$ (a) and 4.22×10^5 at $t=1.87\times10^{-2}$ (b).

of the decay function is needed for elucidating the nature of the line width.

Figure 7 shows the line-width distribution function $G(\Gamma)$ obtained by the histogram method. The average line width $\bar{\Gamma}$ and $\mu_2/\bar{\Gamma}^2$ calculated from the histogram (h) are listed in Table II, along with those from the cumulant method (Cu). Agreement between the two methods is close. $G(\Gamma)$ for the $M_w\geq4.22\times10^5$ has a bimodal distribution at any temperature from Θ to the critical region. The fraction of the fast-mode decreases with decreasing molecular weight, and the correlation function shows a unimodal decay for $M_w\leq1.10\times10^5$. For an intermediate molecular weight $M_w=2.33\times10^5$, both unimodal and bimodal distributions appear in the histogram. In semidilute solutions near the Θ temperature, two modes of motion have been observed by photon correlation spectroscopy.[18] The present analysis shows that the bimodal distribution exists even at the critical concentration and near the critical temperature in higher molecular weight samples. The $\bar{\Gamma}$ of the total correlation function and the average line width for the slow mode had a similar temperature dependence, and no appreciable temperature dependence was found in the fraction of each mode. Thereofre, the existence of two modes seems to have no direct relation to the large background. However, the range of molecular weight treated in this work was not very wide and the fraction of fast mode in $\bar{\Gamma}$ was small (about 10—20% for $M_w=1.26\times10^6$). Hence, further investigations are needed using samples of higher molecular weight.

REFERENCES

1. P. Debye, *J. Chem. Phys.*, **31**, 680 (1959).
2. P. Debye, H. Coll, and D. Woermann, *J. Chem. Phys.*, **32**, 939 (1960); **33**, 1746 (1960).
3. P. G. de Gennes, *Phys. Lett., A*, **26**, 313 (1968).
4. B. Chu, *Phys. Lett., A*, **28**, 654 (1969).
5. N. Kuwahara, D. V. Fenby, M. Tamsky, and B. Chu, *J. Chem. Phys.*, **55**, 1140 (1971).
6. Q. H. Lao, B. Chu, and N. Kuwahara, *J. Chem. Phys.*, **62**, 2039 (1975).
7. M. Nakata, N. Kuwahara, and M. Kaneko, *J. Chem. Phys.*, **62**, 4278 (1975).

8. T. Dobashi, M. Nakata, and M. Kaneko, *J. Chem. Phys.*, **72**, 6685, 6692 (1980).
9. K. Shinozaki and T. Nose, *Polym. J.*, **13**, 1119 (1981); K. Shinozaki and T. Nose, *J. Phys. Soc. Jpn.*, **50**, 1817 (1981).
10. K. Shinozaki, T. Hamada, and T. Nose, *J. Chem. Phys.*, **77**, 4734 (1982).
11. T. Nose and T. V. Tan, *J. Polym. Sci., Polym. Lett. Ed.*, **14**, 705 (1976); K. Shinozaki, T. V. Tan, Y. Saito, and T. Nose, *Polymer*, **23**, 728 (1982).
12. K. Hamano, T. Nomura, T. Kawazura, and N. Kuwahara, *Phys. Rev.*, **A26**, 1153 (1982).
13. K. Kawasaki, *Ann. Phys.*, **61**, 1 (1970).
14. H. L. Swinney and D. L. Henry, *Phys. Rev.*, **A8**, 2586 (1973).
15. D. W. Oxtoby and W. M. Gelbart, *J. Chem. Phys.*, **61**, 2957 (1974).
16. J. P. Munch, G. Hild, and S. Candau, *Macromolecules*, **16**, 71 (1983).
17. P. G. de Gennes, "Scaling Concepts in Polymer Physics," Cornell Univ. Press, Ithaca, N. Y., 1979, Chapter IV, p. 114.
18. T. Nose and B. Chu, *Macromolecules*, **12**, 590 (1979); B. Chu and T. Nose, *ibid.*, **12**, 599 (1979); *ibid.*, **13**, 122 (1980).
19. R. F. Chang, H. Burstyn, and J. V. Sengers, *Phys. Rev.*, **A19**, 866 (1979); A. J. Bray and R. F. Chang, *ibid.*, **A12**, 2594 (1975).
20. H. E. Stanley, "Introduction to Phase Transitions and Critical Phenomena," Clarendon Press, Oxford, 1971, Chapter 7, p 104.
21. D. E. Koppel, *J. Chem. Phys.*, **57**, 4814 (1972).
22. E. Gulari, E. Gulari, Y. Tsunashima, and B. Chu, *J. Chem. Phys.*, **70**, 3965 (1979).
23. J. C. Le Guillou and J. Zinn-Justin, *Phys. Rev. Lett.*, **39**, 95 (1977); *Phys. Rev.*, **B21**, 3976 (1980).